Research Article | Vol. 28, No. 13 / 22 June 2020 / Optics Express 18859
Optics EXPRESS

High-order harmonics generation in the plasmas produced on different rotating targets during ablation using 1 kHz and 100 kHz lasers

GANJABOY S. BOLTAEV,[1,2] RASHID A. GANEEV,[1,3,5] VYACHESLAV V. KIM,[1,4] NAVEED A. ABBASI,[1] MAZHAR IQBAL,[1] AND ALI S. ALNASER[1,6]

[1]*Department of Physics, American University of Sharjah, Sharjah 26666, United Arab Emirates*
[2]*Tashkent Institute of Irrigation and Agricultural Mechanization Engineers, Tashkent 100000, Uzbekistan*
[3]*Faculty of Physics, Voronezh State University, Voronezh 394006, Russia*
[4]*Faculty of Physics, National University of Uzbekistan, Tashkent 100174, Uzbekistan*
[5]*rganeev@aus.edu*
[6]*aalnaser@aus.edu*

Abstract: We analyze the high-order harmonics generation using 1 kHz and 100 kHz lasers by ablating different rotating targets. We demonstrate the high average flux of short-wavelength radiation using the latter laser, while comparing the plasma formation conditions at different pulse repetition rates. The analysis of harmonic stability in the case of the 100 kHz experiments showed the two-fold decay of the 27th harmonic generating in silver plasma after 3.5×10^6 shots. The advantages of shorter pulse–induced ablation for the improvement of harmonic generation stability are demonstrated. Two-color pump of plasma, resonance enhancement of single harmonic, and quasi-phase matching studies are presented for 1 kHz laser applications. The formation of modulated multi-jet plasma on the plane and curved surfaces during ablation by 100 kHz pulses is demonstrated. In the case of the 25th harmonic of 1030 nm radiation (E=30 eV) generated during experiments in carbon plasma, at 100 kHz and 40 W average power of driving pulses, 0.4 mW of average power for single harmonic in the 40 nm spectral range was achieved.

1. Introduction

High-order harmonic generation (HHG) during propagation of ultrashort laser pulses through gases [1] and laser-produced plasmas (LPPs) [2] is a well-developed method for the formation of coherent extreme ultraviolet (XUV) sources. LPPs are considered as media that allow the observation of different physical and optical processes during HHG, which one can hardly realize in the gaseous media. Among them are the resonance-induced enhancement of single harmonic [3], nanoparticle-induced growth of HHG conversion efficiency [4], quasi-phase matching (QPM) in the spatially modulated plasma allowing the enhancement of groups of harmonics in different XUV ranges [5], etc.

Despite these advantages of HHG in LPPs, the application of high-pulse repetition rate lasers gave rise to issues that pertain to the insufficient stability of the formed plasma plumes, which causes a decay of harmonic yield after a few hundred thousand shots on the target surface. This problem does not exist with 10 Hz class lasers. However, when using kHz class driving lasers the formation of craters on the surface of the studied materials, during ablation of the same spot of the target, becomes inevitable. The up-and-down movement of the target can, to some extent, be used for resolving this issue of the instability of plasma characteristics, but cannot alone fully resolve it.

The rotation of target can notably diminish this problem in the case of 1 kHz lasers. In such case, the formation of stable weakly ionized plasmas from laser ablation of solid targets

#393054 https://doi.org/10.1364/OE.393054
Journal © 2020 Received 18 Mar 2020; revised 30 May 2020; accepted 4 Jun 2020; published 9 Jun 2020

Optics EXPRESS

using a 1 kHz pulse repetition rate lasers can be used for stable high-order harmonic generation from plasma plumes [6]. The developed technique allowed achieving the long-term stability of harmonic yield.

The justification in finding optimal procedures for improving the stability of the harmonics generating in LPPs is related to the observations of the advanced properties of plasma harmonics over gas harmonics [7]. Particularly, the HHG conversion efficiency in some plasma plumes was one order of magnitude stronger compared with in-gas HHG efficiency [8]. Earlier reported analysis of plasma formation by pulses of different duration [9] also pointed out the importance in determining the optimal conditions of laser-target interaction in the case of high-pulse repetition rate sources of coherent IR radiation. All these requirements for stability of plasma play exceptionally crucial role in the case of the application of a new generation of lasers operating at two orders of magnitude larger pulse repetition rates (100 kHz and higher).

Here we report the application of rotating targets for LPP formation and HHG at two ranges of pulse repetition rates (1 kHz and 100 kHz). The latter case has never been studied, to the best of our knowledge. We demonstrate the high average flux of short-wavelength radiation using 100 kHz pulses, while comparing the plasma formation conditions at different pulse repetition rates. The advantages of shorter pulses induced ablation for the improvement of harmonic generation stability are demonstrated. The formation of modulated multi-jet plasma on the plane and curved surfaces during ablation by 100 kHz pulses is demonstrated.

2. Experimental arrangements

The experimental setup used in the presented investigations is shown in Fig. 1. The experiments were carried out using two lasers: Ti:Sapphire laser (Spectra Physics Ace) and Yb-doped fiber laser (UFFL_300_2000_1030_300; Active Fiber System) operated at 1 and 100 kHz pulse repetition rates, respectively.

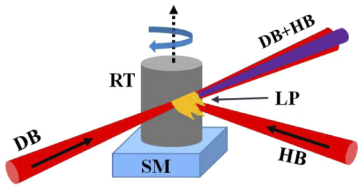

Fig. 1. (a) Experimental setup for HHG using rotating target. DB: femtosecond driving beam, SM: motor, RT: rotating target, HB: picosecond (or femtosecond) heating beam, LP: laser plasma, DB + HB: driving beam and harmonic beam.

In the case of first laser (L1, λ=800 nm), ablation of targets to create the plasma plume was carried out by pulses with durations of 200 ps and 35 fs. In the first case, the heating pulse was created by splitting off a portion (2 mJ) of the uncompressed 200 ps laser pulses and focused by spherical lens on the target surface for plasma formation. The remaining driving pulse was compressed in a compressor and then focused into plasma plumes with 500 mm focusing lens. The driving pulse propagating through LPP was delayed with respect to the ablation pulse by 50 ns to allow the plasma to move away from the target surface to such extent, which allowed converting pulse to pass at the distance of 0.2 mm from the target surface through the densest part of plasma without being clipped by the target. In the second case, the 35 fs pulse was split by two parts, one of which being delayed with regard to other by 50 ns. This combination of two pulses allowed formation of plasma by the first 35 fs pulse with second 35 fs pulse being propagated through the LPP.

In the case of second laser (L2), we used two outputs that the system delivers through two ports. The first port provided 250 fs, 1030 nm, 50–150 kHz, 0.3 mJ pulses that were used for LPP

Optics EXPRESS

formation. The second port provided 37 fs pulses (1030 nm, 50–150 kHz, ~1 mJ), which were used as the driving radiation for harmonics generation. The experiments with this laser were carried out at 100 kHz pulse repetition rate. The target movement and rotation system consisted of three linear stages driven by stepper motors. The target was attached to an axis of the fourth motor, which provided rotation with a variable velocity of rotation (from a few rotations per minute (rpm) up to 150 rpm).

The 250 fs pulses from the first port were directed towards the vacuum chamber and focused using a 300 mm focal length spherical or cylindrical lens on the surface of target. The optimal fluence and intensity of 250 fs heating radiation on the target surface were $F = 0.5$ J cm^{-2} and $I_{hp} = 2\times10^{12}$ W cm^{-2}, respectively. At these conditions of ablation we observed the maximal yield of harmonics from different plasmas. We also used the nanosecond pulses from Nd: YAG laser (5 ns, 1064 nm, 10 Hz, 5 mJ) for ablation of targets using approximately same fluence to determine the optimal delay between heating and driving pulses to increase the harmonic yield, as well as to compare the harmonic yield with regard to the ablation using femtosecond pulses.

We also compared HHG from gases and plasma. The gas jet (diameter of nozzle 0.25 mm) was placed at the focal plane of the focused radiation and operated with a continuous Ar flow at a pressure of 70 mbar.

The harmonic radiation was analyzed by an XUV spectrometer consisting of a cylindrical (or flat) gold-coated mirror, a 1200 lines/mm flat-field grating and an imaging microchannel plate detector with phosphor screen imaged onto a CCD camera. The difference in harmonic yields in the case of different repetition rates of driving and heating pulses was adjusted by varying the collection time of CCD camera. Commonly, this parameter was tuned for comparative analysis of the harmonic yields generated from low and high repetition rate pulses. In the case of the 1 kHz repetition rate experiments, 10 ms integration time of CCD was used, while for 100 kHz case this value was equal to 60 μs. Thus in the case of 1 kHz laser we collected 10 shots for HHG spectrum, while in the case of 100 kHz laser six shots were collected for a single spectrum of harmonics.

The Al, In, Ag, C and Au rods were used for plasma formation on the rotating targets. The targets (cylindrical rods with diameter of 15 mm and length of 30 mm) were installed on the rotating motor as shown in Fig. 1, with the driving pulse propagating at a distance of 100–200 μm above the target surface. We also used silver thin foil wrapped around the stainless steel rod to form the homogeneously ablated areas during the rotation of this target.

3. Results

3.1. Analysis of harmonics stability from the 1 kHz and 100 kHz plasmas

The irradiation of the fresh surface of target by each next pulse is not a necessary requirement for achieving harmonic stability. The heating beams can overlap on the target surface during its rotation until the overheating notably changes the conditions of plasma formation on the corrupted surface. During these studies, we used the rotating targets to exclude or diminish the instability of harmonic yield caused by degradation of the surface during laser ablation. In the case of 1 kHz repetition rate laser, the commonly used rotating speed was varied between 20 and 30 rpm for different targets. This rotation speed allowed achieving the stable harmonic output. However, even at 5 rpm, the stability of harmonic yield was significantly better compared with unmovable target. In the case of 20 rpm speed of targets, approximately 30 pulses overlapped on the same spot.

In the case of ablation using 100 kHz pulses we used the rotating speeds up to 150 rpm for generation of stable harmonics. In that case, approximately 400 laser shots were overlapped on the same spot. At these conditions, the harmonic yield started to gradually decrease after some time from the beginning of ablation. The increase of rotation speed up to 600 rpm did not allow the improvement of harmonic stability. Thus in the case of 100 kHz ablation, the main factor of

Optics EXPRESS

instability was the insufficient flow of heat out from the surface of heated spot. However, the stability improved once we dragged the rotating target up and down. The optimization of this vertical movement of the target allows ensuring reliable continuous generation of harmonics from LPP.

Different harmonic orders can be used for analysis of the stability of harmonic yield. We chose the harmonic order in the mid of the whole spectrum of generated XUV radiation in the plateaulike range (15^{th} to 55^{th} orders). Figure 2(a) shows the variation of 27^{th} harmonic from the Ag plasma produced on the rotating target using 1 kHz, 200 ps, 800 nm heating pulses. The 35 fs pulses from L1 were used as the driving radiation for harmonics generation. The target was rotated at a velocity of 10 rpm. The reasonably good stability, with variations of harmonic yield not exceeding 5%, was maintained for a long time. In the case of abrupt stop of the rotating motor the harmonic was significantly decreased. The moment of motor stopping is shown in Fig. 2(a) by an arrow after 110 s corresponding to 0.11×10^6 laser shots from the beginning of ablation. After that, the harmonic yield was decreased within 10 to 15 seconds down to ~7% compared with the case of rotating target. The change in the target rotation velocity did not lead to a decrease in the harmonic yield as far as this velocity was maintained above 3 rpm. The inset in Fig. 2(a) shows the harmonic spectrum from stable plasma produced on the rotating silver target in the XUV range. The harmonic spectrum was extended up to 55^{th} order (i.e. up to the wavelength of 14.5 nm and photon energy E_{ph} = 85.2 eV).

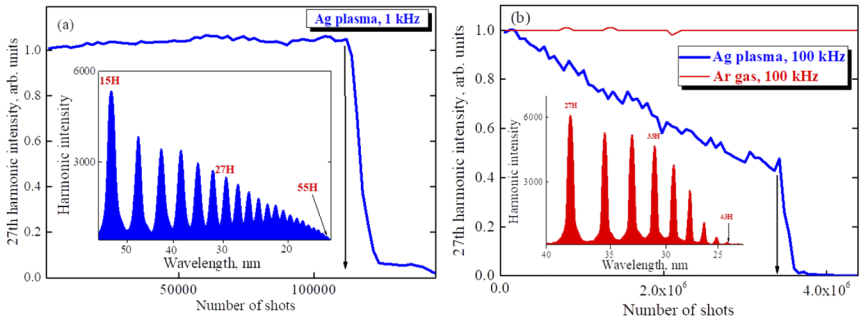

Fig. 2. (a) Stability measurements of the 27^{th} harmonic generating in the silver plasma produced on the target rotating at 5 rpm during 110 s from ablation using 1 kHz, 800 nm, 200 ps pulses (laser L1). The harmonic was abruptly decreased once the motor stopped after 110 s from ablation (shown by the arrow). Inset: HHG spectrum from Ag plasma. (b) Stability measurements of the 27^{th} harmonic generating in Ar gas (red thin curve) and Ag plasma (blue thick curve) produced on the target rotating at 100 rpm during 35 s from the beginning of ablation using 100 kHz, 1030 nm, 250 fs pulses (laser L2). The harmonic was almost disappeared at the moment when the target was stopped (shown by the arrow). Inset: HHG spectrum from Ag plasma.

In the case of L2, the stability of harmonics from LPP was worsened. Figure 2(b) shows the decay of 27^{th} harmonic yield from the plasma produced on the rotating Ag target by 100 kHz pulses within first 35 seconds from the beginning of ablation (blue thick curve) corresponding to 3.5×10^6 shots. When the motor stopped, almost all harmonics disappeared except of a few lowest orders. These experiments were carried out at 100 rpm. The increase of rotation velocity (up to 150 rpm) did not lead to improvement of the stability of harmonic yield, probably, due to the overheating of the target area and craters formation. Meanwhile, the harmonic generation from gas target was stable within the whole set of similar experiments using 100 kHz pulses (red thin curve). The inset in this figure shows the harmonic spectrum from Ag plasma extended up to the 43^{rd} order (λ=23.9 nm, E_{ph} = 51.8 eV). Notice that we achieved higher conversion efficiency of lower-order harmonics in LPPs compared with HHG in argon gas even at the conditions

Optics EXPRESS

when concentration of particles in plasma was lower than in gas (3×10^{17} and 3×10^{18} cm^{-3}, respectively).

The application of 1 kHz laser (L1) for HHG in other LPPs (Au, Al) showed similar features like those presented in Fig. 2(a). The difference between the dynamics of harmonic decay after motor stopping was observed once we used picosecond or femtosecond pulses as the heating radiation. Figure 3(a) shows the decay of the 19th harmonic generated in the Al LPP produced by 35 fs (blue thick curve) and 200 ps (red thin curve) pulses. The decay of 19th harmonic started at the moment when the motor with aluminium rod was stopped (black arrow). One can see that the decay down to 10% of the stable level of harmonic yield was achieved within 7 seconds from stopping the motor in the case of 200 ps heating pulses, while in the case of 35 fs heating pulses this decay was less abrupt (12 s).

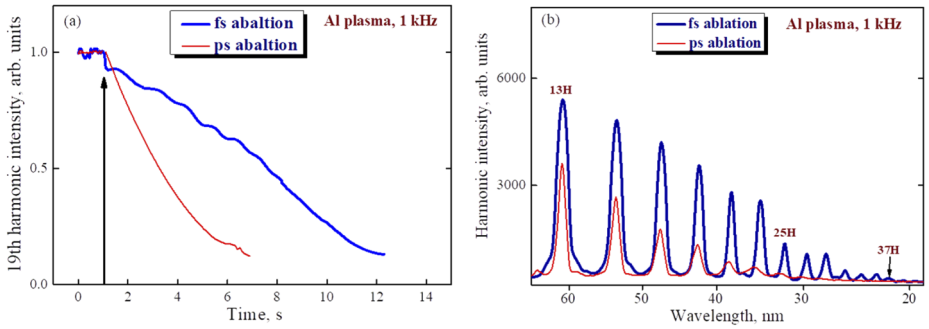

Fig. 3. (a) Decay of the 19th harmonic generated from the Al LPPs produced by 35 fs, 1 kHz pulses (blue thick curve) and 200 ps, 1 kHz pulses (red thin curve) after stopping the motor rotating aluminum rod (shown by arrow). (b) Spectral distribution of the harmonics generated by 800 nm, 35 fs driving pulses in the stable LPP produced on the rotating Al rod using femtosecond (thick blue curve) and picosecond (thin red curve) heating pulses.

The purpose of stopping the rotation of motor was to show how fast the impeding factors originated on the overheated target surface destroy the maintenance of "optimal" plasma in the case of ablation by 200 ps or 35 fs pulses. The motivation of those experiments using 1 kHz heating pulses of different duration was to show that femtosecond pulses lesser modify target surface compared with picosecond pulses at approximately similar fluence of both pulses on the target surface (~1 J cm^{-2}). These findings are even more important for the case of 100 kHz pulses. Earlier report on this decay of harmonics from 1 kHz LPP [6] was aimed in demonstration of the worsening plasma formation conditions in the case of the picosecond ablation of stopped target. During present studies, the difference between the dynamics of harmonic decay was observed once we used either picosecond or femtosecond pulses as the heating radiation from 1 kHz laser. Thus we underline the preference in ablation of rotating target by shorter (35 fs) pulses rather than longer ones (200 ps) at 1 kHz repetition rate. This finding was used during our following experiments with 100 kHz laser when we applied the 250 fs pulses for plasma formation on the target surface.

The observed difference of the harmonic intensity decay after stopping the rotating target can be explained by the depth of the crater formed by different heating pulses, which depends on the duration of the ablating pulses [10,11]. The total heat penetration depth (l) in materials depends on the optical penetration depth (l_a) and thermal penetration depth l_t in metals ($l = l_a + l_t$) and in metals actually equal to l_t, which is mostly determined by pulse duration, $l_t = 2(K_e\tau_p)^{0.5}$ [11]. Here K_e is the heat conductivity due to electrons and τ_p is the pulse duration. The width of the heat-affected zone in metals can be estimated from this relation, as long as laser pulse duration exceeds electron-phonon relaxation time. Shorter pulses reduce this zone and make the ablation

Optics EXPRESS

process more uniform and stable. Meanwhile, the deeper crater in the case of heating picosecond pulses compared to femtosecond pulses causes the worsened conditions for the optimal LPP formation. The results of our studies corroborated with the theoretical consideration of surface modification by different ablating pulses described by above relation.

In Fig. 3(b), the spectra of the harmonic spectra generated in Al LPP using different 1 kHz heating pulses are shown. In the case of ablation by 35 fs pulses, we achieved the extension in the harmonic cutoff energy up to 57.3 eV (λ=21.6 nm, 37H), which was notably larger than the harmonic cutoff observed in aluminum plasma produced by 200 ps pulses (E_{ph} = 38.7 eV, λ=32 nm, 25H). This extension of cutoff can be attributed to the involvement of double charged Al ions with higher ionization potential. Similar extension has earlier been reported in the case of manganese plasma [12].

3.2. *Two-color pump of the plasmas produced on the rotating targets by 1 and 100 kHz pulses*

The two-color pump (TCP) scheme of HHG in LPPs was performed using two orthogonally polarized 800 nm and 400 nm driving pulses (L1) and 1030 nm and 515 nm driving pulses (L2), respectively. In the case of L1, the second harmonic generation (SHG) at λ=400 nm was achieved using a 0.2 mm thick barium borate (BBO) crystal, which was inserted inside the vacuum chamber on the path of the 800 nm fundamental radiation. The SHG conversion efficiency was ~3%, so in the plasma area the ratio of fundamental and second harmonic intensities was 33:1, which corresponded to the 5.7:1 ratio of the amplitudes of fundamental and second harmonic waves. Even this small part of second field allowed generation of almost equal odd and even harmonics.

The example of TCP (800 nm + 400 nm) of the plasma produced on the rotating indium target is shown in Fig. 4(a) (blue dashed curve). We observed the generation of odd and even harmonics up to the 21st harmonic. In the meantime, the application of single-color pump (SCP, 800 nm) at similar conditions (i.e. by removal of BBO from the path of 800 nm beam) led to generation of weaker harmonics (red solid curve). The application of TCP allowed the generation of even harmonics. Some of them (12H, 14H) were close to the ionic transition of indium possessing large oscillator strength, which led to the enhancement of those even harmonics, alongside with H13. Application of Al rotating target for TCP at similar conditions demonstrated the generation of equal gradually decreasing odd and even harmonics (Fig. 4(b), blue dashed curve). HHG using SCP scheme also showed the similar gradually decreased odd harmonics (red solid curve). In both cases (In and Al rod targets) we used picosecond pulses as heating radiation.

Figure 5 shows the raw images of harmonic spectra generated in (a) silver plasma and (b) argon gas in the case of SCP and TCP at 1 kHz pulse repetition rate. The presentation of the images of HHG spectra collected by CCD camera can visually demonstrate various features of this process. These spectra were collected using flat gold-coated mirror in XUV spectrometer, which allowed the analysis of the divergence of high-order harmonics, alongside the observation of the variations of phase matched conditions along the XUV spectra range.

The harmonic spectra at two regimes of pumping (SCP, TCP) of the silver plasma produced on the rotating Ag rod are presented in Fig. 5(a). One can see the enhancement of harmonic yield during SCP of Ag LPP in the case of higher orders of harmonics compared to the lower orders (upper panel). Also we noticed larger divergence of the harmonics belonging to the shorter wavelength range, contrary to the common rule of wavelength-dependent divergence (θ) and sizes (d) of harmonic beam ($\theta(d)$ α λ). This deviation is related to the prevailing influence of the collective effect of phase matching for the shorter-wavelength harmonics, which caused their stronger yield.

Another pattern of harmonic distribution appeared in the case of TCP (bottom panel). One can see the gradually decreased harmonic yield for both odd and even harmonics, alongside with the decrease of divergence for each next harmonic order. One can also admit the significantly larger

Optics EXPRESS

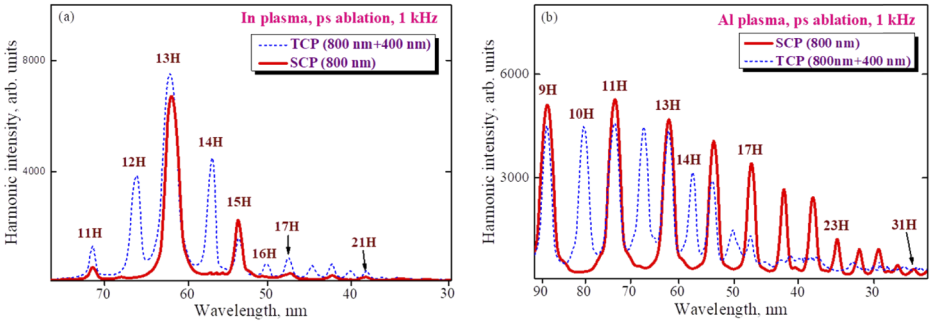

Fig. 4. (a) Spectral distributions of the harmonics generated in the indium plasma using SCP (800 nm) and TCP (800 nm + 400 nm) in the case of 1 kHz laser. Blue dashed curve shows the odd and even harmonics obtained in the case of TCP and red solid curve shows the odd harmonics obtained in the case of SCP. The SHG conversion efficiency in TCP scheme was equal to 3%. (b) Spectral distributions of the harmonics generated in the aluminum plasma using SCP and TCP. Blue dashed curve shows the odd and even harmonics obtained in the case of TCP and red solid curve shows the odd harmonics obtained in the case of SCP.

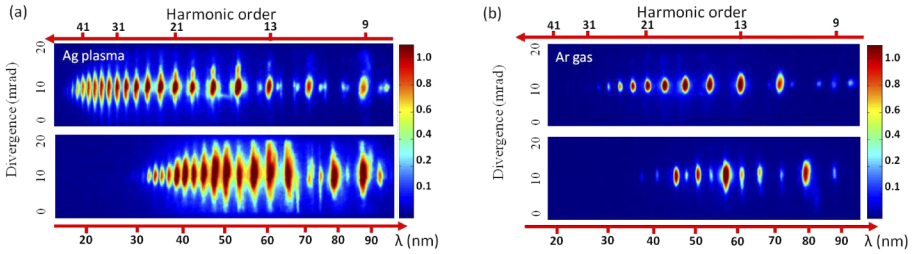

Fig. 5. Raw images of harmonic spectra from LPP and gas using 1 kHz pulse repetition rate. (a) HHG in silver plasma using single color (upper panel) and two-color (bottom panel) pump schemes. (b) HHG in Ar gas using single color (upper panel) and two-color (bottom panel) pump schemes.

harmonic yield in the case of TCP compared with SCP, as well as similar intensities of neighboring odd and even harmonics. This advantage of using TCP has already been demonstrated during HHG studies in gases and plasmas (for example [13,14]). The difference in harmonic divergence can be attributed to the recombination process of ionized electron through the long or short trajectories.

In the case of TCP of silver plasma (bottom panel of Fig. 5(a)), stronger lower order odd and even harmonics gradually decreased towards the shorter wavelength range. These results also underline the significant increase of harmonic yield in the case of the presence of very weak second harmonic field (2 to 6% of the intensity of fundamental wave, depending on the thickness of used BBO crystal), which, in the case of gas HHG, was attributed to the formation of a quasi-linear field and higher ionization rate compared with SCP [13].

We compared these spectra from LPP with those from Ar gas. In the case of SCP (800 nm, Fig. 5(b), upper panel), a gradual decrease of harmonic yield and divergence characterized the behavior of HHG in gaseous medium. The comparison of SCP in plasma and gas media showed the notable prevalence of harmonic yield from the former medium. We maintained approximately similar concentrations of plasma and gas ($\sim 3\times10^{17}$ cm^{-3}) during these experiments and used similar intensities for the driving pulses (2×10^{14} W cm^{-2}). The application of TCP of Ar led to the appearance of even harmonics, which were stronger than the odd ones (bottom panel).

Optics EXPRESS

Application of 100 kHz laser for TCP in plasma also led to significant growth of the harmonic yield compared with SCP. We analyzed the role of second field in the variations of the harmonic intensity generated in the plasmas produced on the rotating targets. Different thicknesses of BBO and velocities of target rotation were used to optimize the harmonic yield. Figure 6 demonstrates different conditions of HHG in the silver plasma produced by 250 fs, 1030 nm, 100 kHz, 0.25 mJ pulses. We used two silver samples: silver bulk rod and thin silver film wrapped around stainless rod to analyze whether heat transfer inside the target depends on the thermal conductivity of samples. SCP of the plasma produced on the bulk rod rotated at 30 rpm led to generation of harmonics only up to the 17th order (Fig. 6(a), upper panel). These conditions of harmonic generation using 1030 nm radiation were notably worse compared with the above-studied case (compare with Fig. 5(a)). The application of 0.1 mm thick BBO allowed generation of a few even orders during TCP of silver plasma (up to 14H, Fig. 6(a), second panel from the top). Though the overlap between 1030 and 515 nm pulses in the area of LPP was perfect in the case of using this thin crystal, the small ratio of the amplitudes of overlapped 515 nm and 1030 nm pulses did not allow the generation of strong odd and even harmonics.

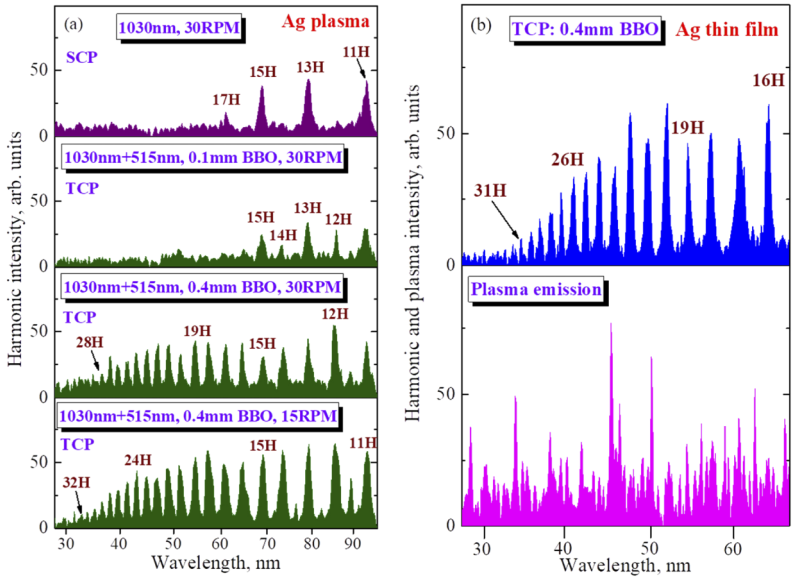

Fig. 6. TCP of silver plasma produced at 100 kHz pulse repetition rate. (a) HHG in the plasma produced on the rotating bulk silver rod. Upper panel corresponds to SCP and 30 rpm of target, while other panels correspond to TCP. Second panel corresponds to TCP using 0.1 mm thick BBO. Two other panels were obtained using 0.4 mm thick BBO at 30 and 15 rpm of bulk Ag rod. (b) Upper panel: HHG using TCP of the plasma produced at a fluence F=1 J cm^{-2} on the silver thin film rounded the stainless steel rod. Approximately similar spectrum was obtained with regard to the Ag bulk rod. Bottom panel shows the plasma spectrum without harmonic emission once stronger excitation of thin film (F=4 J cm^{-2}) leads to significant phase mismatch between the driving (1030 nm and 515 nm) waves and harmonics.

Two bottom panels of Fig. 6(a) were obtained using 0.4 mm thick BBO at 30 and 15 rpm of bulk Ag rod. Third panel demonstrates a significant improvement of odd and even harmonics compared with the application of 0.1 mm thick BBO. SHG efficiencies in these comparative experiments were 1.5% (in the case of 0.1 mm thick BBO) and 4.7% (in the case of 0.4 mm thick BBO). Harmonics up to the 28th order were routinely obtained during this set of studies. The application of thicker crystal for SHG can cause a temporal separation of two pumps (fundamental

Optics EXPRESS

and second harmonic waves) due to group velocity dispersion in BBO. This separation did not allow efficient generation of even harmonics in previous studies using 800 nm fundamental radiation from Ti: sapphire lasers. Meanwhile, in the case of longer wavelength driving sources, like Yb-doped fiber laser, the difference in group velocity dispersion of ω and 2ω waves was smaller, which allowed the application of thicker crystal to produce larger amount of second harmonic photons, while maintaining sufficient overlap with the fundamental radiation in the area of LPP.

We compared HHG at two regimes of rotation velocities in the ablating silver rod (30 and 15 rpm; two bottom panels of Fig. 6(a)). The decrease of rotation speed did not cause the worsening of harmonic stability, but rather improved the harmonic yield and cutoff (up to the 32nd order; bottom panel). To analyze the role of heat removal, we used thin (0.1 mm) silver film. The upper panel in Fig. 6(b) shows HHG spectrum using TCP of the plasma produced on such film. Notice that the thin Ag film was wrapped around a stainless steel rod, but the harmonic yield was the same as for bulk silver (compare bottom panel of Fig. 6(a) and upper panel of Fig. 6(b)), while steel has a much worse thermal conductivity than silver. This observation allowed concluding that the thermal penetration depth has no significant influence on heat dissipation and correspondingly HHG yield.

This assumption can be qualitatively considered when the heat distribution is calculated. Previous study [15] allows to assess the surface temperature after applying the heating pulse. It was pointed our that for the short pulses the widely used surface generation model can give erroneous results compared to the more accurate volume generation model. Newertheless, both models predict the relatively slow flow of heat inside the volume, which has been proven in the case of the tungsten heated by 30 ps pulses. In our case, the application of 250 fs or 200 ps pulses should also lead to the slow decrease of temperature along the depth of material. That is why the expected similarity in surface temperature maps for the bulk and 0.1 mm thick silver may point out the similarity in the plasma formation and harmonic generation, which was proven in our studies of these silver samples. However, the preferable flow of heat along the surface will cause its accumulation in the case of high pulse repetition ablation of the same or nearby place of rotated target and faster modification of the surface compared with 1 kHz laser. One has to note that these estimates seem insufficient to deal with another problem occurring during overheating of the same spot by multiple shots differently overlapped with each other at variable velocities of rotating target. The issue, which can play a decisive role in that case, is the appearance of free electrons in plasma cloud, which can destroy the phase matching conditions.

The conditions of plasma formation were chosen such that maximal yield of odd and even harmonics as well as longevity of stable harmonics generation were achieved. The optimal fluence of heating 250 fs pulses in these conditions was found to be F=1 J cm^{-2}. The increase in fluence led to a decrease of both the stability of harmonic yield and the conversion efficiency. The formation of denser plasma did not compensate the growing influence of free electrons that appeared at these conditions. The free electrons are responsible for the abrupt deviation from the optimal phase matching conditions for efficient HHG in LPP. The bottom panel in Fig. 6(b) shows only plasma emission spectrum at the conditions when stronger excitation of thin film (F=4 J cm^{-2}) led to significant phase mismatch between the driving (1030 nm and 515 nm) waves and the harmonics.

Similar results were obtained using other targets. Figure 7(a) shows the harmonic spectra generated during SCP and TCP of Au LPP using 100 kHz laser. The upper panel demonstrated the harmonic spectrum obtained during SCP of the plasma produced by 250 fs pulses on the surface of gold ring. Two other panels were obtained using TCP of Au LPP when 0.1 and 0.4 mm thick crystals were used for SHG. One can see the similarities of the harmonics generated in gold (Fig. 7(a)) and silver (Fig. 6(a)) plasmas.

Optics EXPRESS

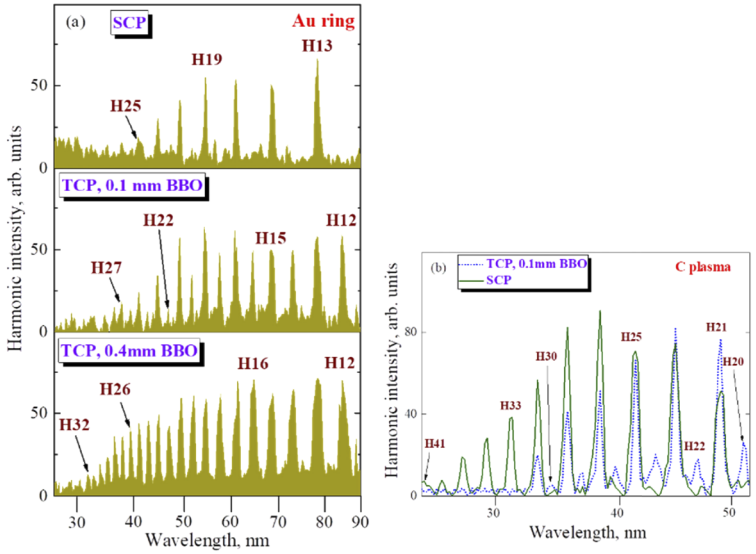

Fig. 7. SCP and TCP of different plasmas using 100 kHz laser. (a) HHG in Au LPP. Upper panel shows the harmonic spectrum obtained during SCP of the plasma produced by 250 fs pulses on the surface of gold ring. Two other panels were obtained using TCP of Au LPP when 0.1 and 0.4 mm thick crystals were used for SHG. (b) HHG in the carbon plasma produced on the graphite rod. The 0.1 mm thick crystal was used for SHG and TCP of C LPP.

The application of soft material (graphite) for HHG worsened the stability of harmonics, while the harmonic yield at these conditions was higher compared to the case of ablated metals. Figure 7(b) presents the SCP- and TCP-induced HHG spectra in the carbon plasma produced on the graphite rod. 0.1 mm thick crystal was used for SHG and TCP of C LPP. Similar to the case of metal plasmas, the weak orthogonally- polarized second field did not improve the whole yield of harmonics and allowed generation of only a few even harmonics, which were notably weaker than the odd ones. However, even in these unfavorable conditions the HHG yield of the lower order harmonics was two to four times stronger compared with metal LPPs. The reasons for appearance of enhanced harmonics in the case of carbon LPP could be attributed to formation of the nanoparticles in plasma, which increased the recombination cross section for the accelerated electrons and correspondingly amended the conditions of harmonic generation. The presence of nanoparticles during these experiments was confirmed during analysis of the debris from ablated graphite deposited on the nearby substrates.

The main goal of this work was to demonstrate the harmonic generation from the plasmas produced by 100 kHz class laser. However, independently on which pulse repetition rate used, the principles of optimal plasma formation are similar for the single shot, 10 Hz, 1 kHz, 100 kHz, etc., cases. The term “optimal” refers to the conditions when the driving beam propagates through the maximally dense plasma arriving on the pass of driving pulse, with minimal factors decreasing harmonic conversion efficiency. The requirements to minimize the impeding factors, such as phase mismatch, strong incoherent plasma emission and additional thermal loading on the target surface, remain same for each of abovementioned regimes of pulse repetition rate. One of the most important issues here is determination of the optimal delay between heating and driving pulses. Once the same laser is used for heating of target by the part of radiation followed with the convertion of femtosecond laser pulses in plasma, the delay between these pulses becomes established by using the variable difference in the distances of propagation of the

Optics EXPRESS

heating and driving beams towards the target. This is a very inconvenient procedure requiring the constant re-adjustment of experimental scheme while adding some extension on the driving beam pass in the case of using materials with different atomic weight.

Most convenient option to define the optimal delay for different ablating materials is the application of the second source, like nanosecond Nd:YAG laser, digitally synchronized with the main laser. The application of such scheme allowed precisely determining the optimal delay between heating and driving pulses to achieve the maximal harmonic yield from the materials possessing different atomic weight. The synchronization of two laser system allows controlling the optimal conditions of HHG in laser-produced plasmas by changing the delay between heating and driving pulses using digitally controlled facility rather than by applying the optical delay between pulses used in previous studies, which does not allow the dynamic variation of delay during experiments. The key feature of the used two-laser configuration is a possibility to control the delay between heating nanosecond pulses and driving femtosecond pulses over long timescale (up to a few hundred microsecond, which is important once one uses complex molecules and large nanoparticles as targets) using the digital delay generator (DG535, Stanford Research Systems). The delay between the heating and driving pulses was monitored on an oscilloscope using a fast photodiode. We determined the optimal delays (50, 75, 150, 150, and 220 ns) in the case of C, Al, Ag, In, and Au plasmas respectively. The knowledge of best delay between pulses for different targets obtained during these studies was then applied during HHG in different plasmas using a single laser, when we adjusted the delay between heating (250 fs or 200 ps) and driving (35 fs) pulses using optical delay.

The additional task considered during these two-laser studies was the comparison of the "nanosecond" and "femtosecond" plasmas as the media for HHG. In the case of 100 kHz laser, we used the nanosecond pulses from Nd: YAG laser (5 ns, 1064 nm, 10 Hz, 5 mJ) for ablation of targets by applying approximately same fluence to compare the harmonic yield with regard to the ablation using femtosecond pulses. Our studies showed that the use of shorter pulses for ablation leads to better conditions of plasma formation, as well as lesser plasma emission, allowing the achievement of stronger harmonic yield at similar conditions of experiments. These studies confirmed the earlier reported results of harmonic generation in the plasmas produced by femtosecond and nanosecond pulses [9].

3.3. Quasi-phase matching in the plasmas produced on the rotating targets

This method is based on the formation of conditions, when the coherent length of some harmonic and a few surrounding ones becomes equal to the sizes of single plasma jet from multi-jet LPP. The enhancement of a group of higher-order harmonics in plasmas due to formation of QPM conditions has been demonstrated and analyzed using different approaches [16–18]. Most of above QPM studies in LPPs were carried out using low pulse repetition rate lasers (10 Hz). It is obvious that the 1 kHz and higher class lasers provide an opportunity for enhancing the average power of the shorter wavelength components in the generated harmonics.

To create multi-jet plasma, the heating pulses from L2 (250 fs, 100 kHz) were focused using cylindrical lens. We installed the stainless steel mesh (sizes of open areas 1×1 mm^2) in front of cylindrical lens to modulate the spatial shape of focused heating beam. The first set of experiments was carried out using the aluminum plane target.

The dynamics of plasma plumes ablated using femtosecond and nanosecond heating pulses is very important for achieving the efficient HHG in plasma plumes. The ICCD camera (Andor) allowed analyzing the dynamics of plasma formation and spreading out from the target surface. We used the 20 ns frame gate and measured the position and emission of plasma at the moments of 0, 20, 40, 60 ns, etc. from the beginning of ablation, while also varied the gate and acquisition time from target to target. Figure 8(a) presents the plasma images at 18, 50, 80, 100, and 400 ns from the beginning of ablation. Those images were obtained during ablation by single pulse of

Optics EXPRESS

100 kHz laser. The left image shows the spreading plasma during ablation of Al plane surface by cylindrically focused imperforated beam, while other images show the shapes of multi-jet plasmas at different time scales from the beginning of ablation. Based on these plasma maps, we determined 50 and 80 ns delays between heating and driving beams as the most suitable for the driving pulse to efficiently interact with the densest part of LPP.

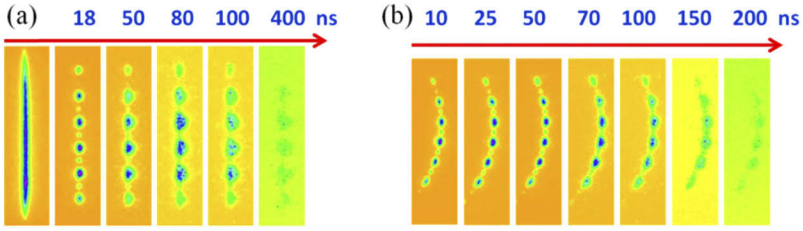

Fig. 8. Images of imperforated and perforated LPPs produced by 100 kHz, 250 fs pulses on the plane and curved surfaces of aluminum. (a) Images of spreading plasma during ablation of Al plane surface by cylindrically focused imperforated beam (left panel) and perforated beam at different delays from the beginning of ablation (other panels). (b) Images of spreading plasma during ablation of rotating Al rod by cylindrically focused perforated beam at different delays from the beginning of ablation.

In the case of extended imperforated plasma, HHG will be suppressed due to the phase mismatch between interacting waves since the length of the excited plasma containing large amount of free electrons is much longer than the coherence length of highest-order harmonics (i.e., the propagation length required for the phase mismatch to reach π). These conditions cause the notable decrease or even full vanishing of those harmonics. The division of such extended plasma on the group of jets equidistantly separated from each other (second to sixth images in Fig. 8(a)) leads to formation of the optimal phase matching conditions between the driving harmonic waves for some orders while maintaining high concentration of plasma components allowing larger conversion efficiency for the specific harmonic. Tose images were taken using the digital generator to control the delay between the heating 250 fs pulses and triggering time of ICCD camera.

As has already been underlined, the application of the static plane target for plasma HHG is not suitable due to overheating of target surface during application of 100 kHz heating pulses. Because of this we also analyzed the perforated plasma jets formed on the rotating targets to determine the conditions of the optimal anlation of targets to create suitable multi-jet plasmas. Figure 8(b) demonstrates the images of spreading plasma during ablation of Al rod surface by cylindrically focused perforated beam at different delays from the beginning of ablation. Such geometry of curved plasma jets was used for the HHG at the conditions of QPM in the case of 1 kHz laser source. Notice that formation of similar conditions for demonstration of QPM in the case of 100 kHz laser source is still under investigation and optimization due to above-mentioned obstacles in stabilization of plasma formation.

The following set of studies shows the enhanced harmonics in the shorter wavelength range of XUV from the plasmas suitable for QPM once one uses the multi-jet LPP produced on the rotating target instead of the extended imperforated plasma formations.

Figure 9 shows the setup and results of HHG experiments using multi-jet plasmas produced by 1 kHz, 200 ps pulses on the rounded surface. The experimental scheme shown in Fig. 9(a) explains how the driving pulse propagates through the imperforated plasma (left panel) and the set of plasma jets (right panel) produced on the rotating rod. In the latter case, different multi-slit masks (sizes of slits 0.5×0.5 mm or 0.2×0.2 mm) were installed in front of the cylindrical lens. Two sets of HHG spectra from modulated (blue dotted curve) and imperforated (red solid curve)

Optics EXPRESS

indium LPP produced by 1 kHz pulse repetition rate laser are shown in Fig. 9(b). As already mentioned, indium plasma allows the resonance-induced enhancement of a single low-order (H13) harmonic of 800 nm radiation, while significantly suppressing the higher-order ones (Fig. 4(a)). In described QPM studies, the resonantly enhanced 13th harmonic was normalized for two cases of imperforated and perforated plasmas. One can see the following gradual decrease of harmonic orders, with harmonic cutoff at 31st order, in the case of imperforated plasma (Fig. 9(b), red thick solid curve). The envelope of harmonic spectrum drastically changed once the extended plasma was replaced by the multi-jet one using the 0.5×0.5 mm multislit mask (Fig. 9(b), blue dotted curve). The enhanced 13th harmonic remained to be the strongest one along the whole set of harmonics, while the notable growth of higher orders centered at around of 23H was observed. The enhancement factor of up to 18× was achieved for the group of harmonics in the spectral range of 20-40 nm.

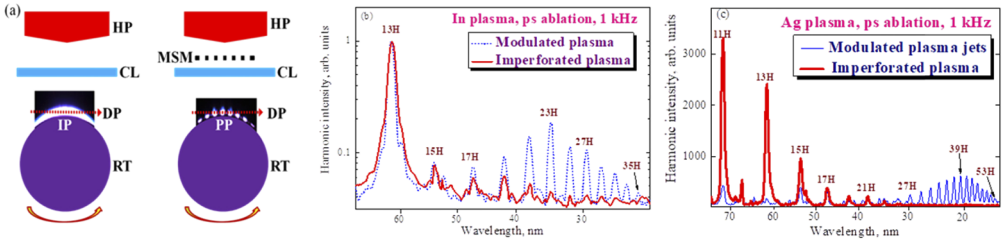

Fig. 9. HHG using multi-jet plasmas produced by 1 kHz laser. (a) Experimental scheme. Left pattern: HP, heating pulse; CL, cylindrical lens; DP, driving pulse; IP, imperforated plasma; RT, rotating target. Right pattern: HP, heating pulse; MSM, multi-slit mask; CL, cylindrical lens; DP, driving pulse; PP, perforated plasma; RT, rotating target. (b) HHG spectra from modulated (blue dotted curve) and imperforated (red solid curve) indium LPP produced on the rotating target. Resonantly enhanced 13th harmonic was normalized for two cases. The enhancement factor up to 18× was achieved for the group of harmonics in the spectral range of 20-40 nm. (c) HHG spectra from modulated (blue thin curve) and imperforated (red thick curve) silver LPP produced by 1 kHz pulse repetition rate laser on the rotating target. The enhancement factor of up to 44× was achieved for the group of harmonics centered at the wavelength of 20 nm.

Similar features of HHG spectra from modulated (blue thin curve) and imperforated (red thick curve) silver LPP are shown in Fig. 9(c). In that case we used the 0.2×0.2 mm mask allowing the extension of the group of enhanced harmonics to the shorter wavelength region. One can see that, in the case of multi-jet plasma, the enhanced harmonics were observed in the spectral range where almost no harmonic emission was obtained in the case of extended imperforated plasma. Notice the decrease in the yield of low-order harmonics from multi-jet plasma. Meanwhile, the enhancement factor of up to 44× was achieved for the group of harmonics centered at the wavelength of 20 nm.

Silver plasma is a very attractive medium for generation of harmonics up to the sixties orders of 800 nm laser radiation. The increase of the fluence of heating pulses causes a two-sided effect on the harmonic distribution and harmonic intensity. Firstly, higher-order harmonics disappear from the spectra of collected emission, and secondly, lowest order harmonics increase with regard to the above-described "optimal" plasma conditions. In that case the harmonic distribution looks like the one shown in Fig. 9(c) (red thick curve). Notice that H11 – H17 harmonics in this spectrum are notably (up to ten to twenty times) stronger than those obtained in the case of "optimal" plasma. The reason for the drop of the intensity of highest order harmonics is an appearance of large amount of free carriers (electrons) dramatically changing the phase matching conditions for those harmonics, while maintaining the affordable conditions for the lower-order

Optics EXPRESS

harmonics. In other words, the coherence length for higher orders becomes notably smaller with regard to the coherence length for the lower orders. Thus at the fixed length of plasma, only lower orders become enhanced in the denser plasma.

The question arises how to maintain the generation of strong higher order harmonics at these conditions of over-heated target? The answer is the use of extended dense plasma, which is spatially modulated in such a way that the modulation period coincides with the coherence length of high-order harmonics. In that case, the group velocities of fundamental and harmonic waves become equal to each other only in a relatively narrow range of XUV spectrum. Correspondingly, these conditions cannot be considered as the phase matched conditions along the whole studied spectral range but rather for a part of it. That is why these conditions of harmonic generation were classified as the nearly ("quasi") phase matching suitable only for the specific XUV range, rather than for the whole region of harmonics generation.

Thus QPM refers to the conditions when the phase matching between interacting waves occurs only in a relatively narrow spectral range of harmonics generation. In that case the harmonics lying out of this region are notably suppressed compared with the case of QPM-free conditions, while the group of harmonics centered at the wavelength of some of them became strongly enhanced (thin blue curve in Fig. 9(c)). To demonstrate this effect, one has to use a strong ablation of target, when in spite of larger concentration of plasma the high concentration of free electrons causes a notable suppression of all harmonics, especially higher order ones.

As we mentioned, the difficulties encountered during experiments with 100 kHz laser, particularly the proper stabilization of plasma parameters, which is especially crucial in the case when collective effects play a decisive role in HHG, did not allow us achieving the stable QPM effect in the case of 100 kHz laser. The stable enhancement of a group of few harmonics was suppressed by target degradation.

Our studies (Figs. 9(b) and 9(c)) confirmed that the curved shape of multi-jet plasma did not prevent demonstration of QPM, thus showing that variable density of different jets interacting with driving pulse is not an unavoidable obstacle, which prevents the coherent addition of harmonics from different areas of rounded perforated ablation. The enhancement factors of QPM-enhanced harmonics in the case of curved jet structures were only slightly smaller compared with parallel multi-jet structures. This observation points out the limited amount of jets involved in collective accumulating process of HHG allowing demonstration of the quadratic dependence of harmonic yield on the number of separated plasma jets. To overcome the problem of heterogeneous distribution of plasma density along the propagation of driving beam nearby to the rotating target, one can modify the position of the rotating motor in such a way that its axis becomes parallel to the direction of driving beam propagation, like it was demonstrated in [5].

4. Discussion

The main goal of this study was the analysis of the high-order harmonics generation in different plasmas produced using 1 kHz and 100 kHz laser sources. The advantages of plasma HHG over gas HHG have been demonstrated during last decade in numerous laboratories. The distinction of former approach over latter one is not only the advantage in conversion efficiency demonstrated by different research teams [3–5], but rather the availability in studies of new optical processes, which were discovered during harmonics generation in plasmas and could not be realized, at least until now, using gases as the media for HHG. Those include the resonance-induced enhancement of single harmonic in different plasmas and applications of nanoparticles and quantum dots for enhancement of harmonics. Meanwhile, the most important issue differing gas and plasma media as the environment for harmonics generation is not the availability of formation of the coherent XUV sources of emission, since similar sources are currently developed by different means, like X-ray lasers and free-electron laser-based technologies, but rather the availability in analysis of the optical and physical properties of almost all non-radioactive solid elements of periodic

Optics EXPRESS

table through their transfer in the plasma state. Notice that, in the case of gas HHG, only a few noble and molecular gases could be used for these purposes, contrary to a few thousand complex solids, which notably increases the activity in the field of atomic physics, optics, and nonlinear spectroscopy of those species.

A significant advantage of gas HHG is the availability in demonstration of the attosecond timescale of harmonic pulses, though some early experiments (for example [19]) have demonstrated that the plasma-induced harmonics can also be considered as attosecond pulses. Notice that most previous attempts in measurements of pulse duration in the case of plasma HHG experiments were stalked due to the problem in delivering a suitable amount of harmonic shots for the analysis of their temporal characteristics. The larger stability of gas harmonics compared with plasma ones allows carrying out these measurements within a few ten minutes. Particularly, an attosecond streaking scan can be done in about 20 minutes at 1 kHz pulse repetition rate. This time span is difficult to maintain for stable harmonic generation in the case of ablation using such lasers. Meanwhile, if one uses 100 kHz laser then it should be possible to do these attosecond streaking scans within 0.2 minutes, assuming flux levels similar to gas harmonics. So 35 seconds of relatively stable harmonic yield demonstrated in present studies, which diminishes only by two times during this time span, should be enough for attosecond streaking scans. Notice (a) the higher conversion efficiency of harmonics from plasmas compared with gases and (b) larger driving pulse energy of the used 100 kHz source with regard to earlier reported 100 kHz gas HHG experiments, when fewer photons per laser pulse compared to a higher pulse energy 1 kHz laser were employed for the attosecond streaking scans. These two advantages can also support the temporal characterization and applications of plasma harmonics.

It is obvious that the HHG efficiency depends on the plasma density, laser pulse parameters (intensity, pulse duration, contrast, focusability, etc.), background ionization, composition of the medium, etc. These parameters cannot be exactly reproduced in different experimental setups with different driving laser sources. However, previous experiments show that the ratio between the harmonic yields from different plasmas remains approximately same even when being studied in different laboratories. The density of the plasma in our 100 kHz experiments was optimized to provide a maximum harmonic yield. Our estimates of conversion efficiency (10^{-5}) approximately match with previous studies [20]. Correspondingly, in the case of the 25^{th} harmonic of 1030 nm radiation (λ=41.2 nm, E=30 eV) generated during present experiments in carbon plasma, at 100 kHz and 40 W average power of driving pulses, 8×10^{13} XUV photons per second were emitted.

The measurements of conversion efficiency of high-order harmonics ($\sim10^{-5}$) from silver LPP in the plateau region have also been reported in [21]. Thus we assumed that in our present studies the 10^{-5} conversion efficiency for the harmonics in the plateau region was achieved. This value refers to a single harmonic in this XUV region. Another estimate of conversion efficiency is related with the comparison of the yields of harmonics from plasmas and gases in a single set of studies. In our case, the intensity of harmonics from plasmas was at least one order of magnitude higher than the one obtained from argon gas at similar laser intensities and particle densities. By assuming the frequently reported efficiency of this process in argon ($\sim10^{-6}$) one can estimate the 10^{-5} conversion efficiency for plasma harmonics. Thus, at 40 W average power of driving pulses used in present studies, the average power of single harmonic was 10^5 times smaller, i.e. equal to 0.4 mW.

5. Conclusions

In conclusion, we have analyzed the high-order harmonics generation using 1 kHz and 100 kHz lasers by ablating different rotating targets. We have demonstrated the high average flux of coherent short-wavelength radiation using latter laser, while comparing the plasma formation conditions at different pulse repetition rates. The analysis of harmonic stability in the case of 100 kHz experiments has shown the two-fold decay of the 27^{th} harmonic generating in silver

Optics EXPRESS

plasma after 3.5×10^6 shots, while no decay in harmonic yield was observed in the case of 1 kHz ablation. Two-color pump of plasma, resonance enhancement of single harmonic, and quasi-phase matching scheme were presented in the case of 1 and 100 kHz pulse repetition rates of target ablation. The formation of modulated multi-jet plasma on the plane and curved surfaces during ablation by 100 kHz pulses has been demonstrated. In the case of the 25th harmonic of 1030 nm radiation (E=30 eV) generated during experiments in carbon plasma, at 100 kHz and 40 W average power of driving pulses, 0.4 mW of average power in the 40 nm spectral range was achieved.

Notice that present work is a first step towards the formation of the stable plasma plume using 100 kHz class lasers, which needs additional efforts for maintaining stable harmonic yield from such laser-produced plasma. We would like to mention the incompleteness in resolving the stability issue for generating harmonics in the case of 100 kHz plasma. The possible scenarios to overpass this issue by dragging the target up and down, alongside with target rotation at optimal velocity, are suggested. Our preliminary experiments with manually movable target (e.g. by pressing and releasing the target holder from the top of vacuum chamber) have shown the perspective in stability improvement for harmonic generation from high-pulse repetition rate plasma. The following plans include the programmable movement of rotating target up and down, which can further diminish the instability issue.

Funding

American University of Sharjah (Common Research Facility, Open Access Program, FRG AS1801).

Acknowledgments

The work in this paper was supported, in part, by the Open Access Program from the American University of Sharjah. This paper represents the opinions of the authors and does not mean to represent the position or opinions of the American University of Sharjah.

Disclosures

The authors declare no conflicts of interest.

References

1. P. B. Corkum, "Plasma perspective on strong field multiphoton ionization," Phys. Rev. Lett. **71**(13), 1994–1997 (1993).
2. Y. Akiyama, K. Midorikawa, Y. Matsunawa, Y. Nagata, M. Obara, H. Tashiro, and K. Toyoda, "Generation of high-order harmonics using laser-produced rare-gas-like ions," Phys. Rev. Lett. **69**(15), 2176–2179 (1992).
3. Z. Abdelrahman, M. A. Khohlova, D. J. Walke, T. Witting, A. Zair, V. V. Strelkov, J. P. Marangos, and J. W. G. Tisch, "Chirp-control of resonant high-order harmonic generation in indium ablation plumes driven by intense few-cycle laser pulses," Opt. Express **26**(12), 15745–15758 (2018).
4. L. B. Elouga Bom, Y. Pertot, V. R. Bhardwaj, and T. Ozaki, "Multi-μJ coherent extreme ultraviolet source generated from carbon using the plasma harmonic method," Opt. Express **19**(4), 3077–3085 (2011).
5. M. Wöstmann, L. Splitthoff, and H. Zacharias, "Control of quasi-phase-matching of high-harmonics in a spatially structured plasma," Opt. Express **26**(11), 14524–14537 (2018).
6. C. Hutchison, R. A. Ganeev, T. Witting, F. Frank, W. A. Okell, J. W. G. Tisch, and J. P. Marangos, "Stable generation of high-order harmonics of femtosecond laser radiation from laser produced plasma plumes at 1 kHz pulse repetition rate," Opt. Lett. **37**(11), 2064–2066 (2012).
7. R. A. Ganeev, G. S. Boltaev, V. V. Kim, M. Venkatesh, and C. Guo, "Comparison studies of high-order harmonic generation in argon gas and different laser-produced plasmas," OSA Continuum **2**(8), 2381–2390 (2019).
8. Y. Pertot, L. B. Elouga Bom, V. R. Bhardwaj, and T. Ozaki, "Pencil lead plasma for generating multimicrojoule high-order harmonics with a broad spectrum," Appl. Phys. Lett. **98**(10), 101104 (2011).
9. R. A. Ganeev, M. Suzuki, M. Baba, and H. Kuroda, "High-order harmonic generation from laser plasma produced by pulses of different duration," Phys. Rev. A **76**(2), 023805 (2007).
10. B. N. Chichkov, C. Momma, S. Nolte, F. Alvensleben, and A. Tünnermann, "Femtosecond, picosecond and nanosecond laser ablation of solids," Appl. Phys. A **63**(2), 109–115 (1996).

Optics EXPRESS

11. F. Brygo, C. Dutouquet, F. Le Guern, R. Oltra, A. Semerok, and J. M. Weulersse, "Laser fluence, repetition rate and pulse duration effects on paint ablation," Appl. Surf. Sci. **252**(6), 2131–2138 (2006).
12. R. A. Ganeev, L. B. Elouga Bom, J.-C. Kieffer, and T. Ozaki, "Demonstration of the 101st harmonic generated from a laser-produced manganese plasma," Phys. Rev. A **76**(2), 023831 (2007).
13. I. J. Kim, G. H. Lee, S. B. Park, Y. S. Lee, T. K. Kim, C. H. Nam, T. Mocek, and K. Jakubczak, "Generation of submicrojoule high harmonics using a long gas jet in a two-color laser field," Appl. Phys. Lett. **92**(2), 021125 (2008).
14. R. A. Ganeev, V. V. Strelkov, C. Hutchison, A. Zaïr, D. Kilbane, M. A. Khokhlova, and J. P. Marangos, "Experimental and theoretical studies of two-color pump resonance-induced enhancement of odd and even harmonics from a tin plasma," Phys. Rev. A **85**(2), 023832 (2012).
15. J. Bechtel, "Heating of solid targets with laser pulses," J. Appl. Phys. **46**(4), 1585–1593 (1975).
16. R. A. Ganeev, V. Tosa, K. Kovács, M. Suzuki, S. Yoneya, and H. Kuroda, "Influence of ablated and tunneled electrons on quasi-phase-matched high-order-harmonic generation in laser-produced plasma," Phys. Rev. A **91**(4), 043823 (2015).
17. V. V. Strelkov and R. A. Ganeev, "Quasi-phase-matching of high-order harmonics in plasma plumes: theory and experiment," Opt. Express **25**(18), 21068–21083 (2017).
18. P. V. Redkin, R. A. Ganeev, and C. Guo, "Analytical treatment of quasi-phase matching of high-order harmonics in multijet laser plasmas: influence of free electrons between jets, intrinsic phase, and Gouy phase," J. Phys. B: At., Mol. Opt. Phys. **52**(7), 075601 (2019).
19. L. B. Elouga Bom, S. Haessler, O. Gobert, M. Perdrix, F. Lepetit, J.-F. Hergott, B. Carré, T. Ozaki, and P. Salières, "Attosecond emission from chromium plasma," Opt. Express **19**(4), 3677–3685 (2011).
20. R. A. Ganeev, "Involvement of small carbon clusters in the enhancement of high-order harmonic generation of ultrashort pulses in the plasmas produced during ablation of carbon-contained nanoparticles," Opt. Spectrosc. **123**(3), 351–364 (2017).
21. R. A. Ganeev, M. Baba, M. Suzuki, and H. Kuroda, "High-order harmonic generation from silver plasma," Phys. Lett. A **339**(1-2), 103–109 (2005).